



Published in final edited form as:

J Surg Res. 2010 January ; 158(1): 147–154. doi:10.1016/j.jss.2008.07.045.

Blood Flow in the Foreign-Body Capsules Surrounding Surgically Implanted Subcutaneous Devices

Carlo R. Bartoli, M.L.A. and John J. Godleski, M.D.

From: Molecular and Integrative Physiological Sciences Program, Department of Environmental Health, Harvard School of Public Health, Boston, MA (CRB, JJG); and Brigham & Women's Hospital, Boston, MA (JJG).

Abstract

BACKGROUND—Surgically implanted devices initiate inflammatory mechanisms and wound healing events and result in the formation of a thick fibrotic capsule that surrounds the device. To investigate the foreign-body response to devices of clinically relevant size, we used microspheres to determine regional blood flow patterns in the foreign-body capsule (FBC) and surrounding subcutaneous tissue after device implantation.

MATERIALS and METHODS—In 10 canines, we implanted 40 subcutaneous devices (polysulfone $n=20$, silicone-coated $n=10$, titanium $n=10$). Via thoracotomy, animals were instrumented with left atrial and aortic vascular access catheters for serial microsphere injections and reference blood sampling. Regional blood flow was repeatedly determined in the FBC, subcutaneous fascia surrounding the FBC, and subcutaneous fascia distal to the surgical site up to 19 weeks after device implantation ($n= 55$ determinations).

RESULTS—As compared to normal blood flow in subcutaneous fascia distal to the surgical site, blood flow increased in FBCs surrounding each device material (polysulfone $p=0.0035$, silicone-coated $p<0.0001$, titanium $p<0.0001$). Additionally, blood flow increased in the subcutaneous fascia within half a centimeter of fibrous capsules encasing polysulfone ($p=0.0035$) but not silicone ($p=0.3706$) or titanium ($p=0.8160$) devices. The time-course of measured blood flow changes within FBCs were similar for polysulfone and silicone but not for titanium.

CONCLUSIONS—Surgically implanted subcutaneous devices of clinically relevant size elicit increases in blood flow in the FBC as well as surrounding fascia. Device material may influence regional blood flow patterns.

Keywords

subcutaneous; microsphere; blood flow; foreign-body capsule; foreign-body response; surgical device

© 2009 Elsevier Inc. All rights reserved.

Address for correspondence: Carlo Bartoli M.L.A., University of Louisville Health Sciences Center, Department of Surgery, Cardiothoracic, Cardiovascular Innovation Institute, 302 E. Muhammad Ali Blvd., 4th Floor, Louisville, KY, 40202, Phone: 502-852-2074, Fax: 502-852-1795, crbart02@louisville.edu.

Publisher's Disclaimer: This is a PDF file of an unedited manuscript that has been accepted for publication. As a service to our customers we are providing this early version of the manuscript. The manuscript will undergo copyediting, typesetting, and review of the resulting proof before it is published in its final citable form. Please note that during the production process errors may be discovered which could affect the content, and all legal disclaimers that apply to the journal pertain.

Introduction

Recent advances in biomaterials and implantable synthetic devices have become increasingly useful in clinical medicine as they often permit outpatient treatment for what would otherwise require hospitalization. With the development of new implantable artificial organs, port/catheter systems, biosensors, power-packs, and orthopedic prostheses, it has become increasingly important to understand the pathophysiological response of tissue to implanted biomaterials and devices of clinically relevant size.

The presence of a foreign body in a physiological environment elicits a cascade of inflammatory mechanisms and wound healing events. Normally, tissue surrounding the implant forms a thick fibrotic pocket referred to as the foreign-body capsule (FBC). This capsule surrounds the device within 7–14 days and continues to accumulate, remodel, and condense over a period of 2 months [1–3]. The capsule acts as both a structural and biological barrier between the tissue and the foreign body. The nature and thickness of the fibrotic capsule is highly sensitive to physical characteristics of the implanted object such as material, size, shape, microgeometry, porosity, and specific molecular moieties of the material [2,4–8]. These characteristics of the device may predispose surrounding tissue to common complications such as inflammation, infection, and tissue necrosis, each of which can lead to impaired device function and/or device rejection.

To better understand the process of bioacceptance and FBC formation, it is important to understand pathophysiological changes in tissue surrounding implanted devices. In relationship to biomaterials and implants of millimeter dimension or smaller, investigators have quantified histological characteristics of the FBC such as thickness [1,7,9–11], collagen content and density [1,5,7,11] fibrinogen content [12], cell composition [7,11,13–15], size and extent of vessel formation [7,10], general inflammatory response [11], and have made semi-quantitative measurements of blood flow [16]. However, no study of which we are aware has directly quantified blood flow in the FBC surrounding implanted devices of clinically relevant size.

With this goal in mind, we developed an *in vivo*, chronically instrumented, conscious canine model to measure regional blood flow in subcutaneous FBCs and surrounding adipose tissue. During the course of this study, we implanted commercially available polysulfone, silicone-coated, and titanium devices to test the hypothesis that individual biomaterials elicit quantifiably different blood flows in the FBC. After the development of the fibrous capsule, we used standard microsphere techniques to determine regional blood flow in the FBC, fascia immediately surrounding the fibrous capsule, as well as unaltered subcutaneous fascia distal to the surgical site.

Methods

Surgical Preparation

All animals received humane care and were handled in accordance with National Institutes of Health and Harvard Medical School animal care committee guidelines. Experimental procedures followed animal study protocols approved by the Harvard Medical Area Standing Committee on Animal Welfare and Use.

Ten adult female mixed-breed dogs, weighing an average of 15.7 kg (range: 14.2–18.2), were used for this study. Instrumentation surgeries were performed aseptically while animals were maintained under a surgical level of anesthesia.

As we have previously described [17–19], animals were instrumented with subcutaneous vascular access port (VAP)/catheter systems to receive multiple injections of different colors of fluorescent-labeled polystyrene microspheres for repeated regional blood flow determinations in the same conscious animal. Via thoracotomy, a vascular access catheter was implanted 4cm into the left atrial appendage so that the catheter tip resided inside of the left atrium. A second vascular access catheter was advanced 10cm and oriented downstream so that the catheter tip resided inside the lumen of the aorta. Catheters were tunneled from the thoracotomy incision, attached to subcutaneous VAPs (n= 20 Polysulfone GPVu, diameter=3.25cm, height=1.25cm; 10 Titanium GPVu, diameter=2.5cm, height=1cm; Access Technologies, Skokie, IL), and buried subcutaneously at the mid-back in multi-layers (Figure 1). VAPs served a dual purpose: 1) for delivery of microspheres into the systemic arterial tree and 2) as the implanted test device. Additionally, silicone-coated telemetry devices (D70-PCT, diameter=5.5cm, height=1.25cm; Data Sciences International, St. Paul, MN) were implanted subcutaneously at the lateral base of the back.

After surgery, animals recovered for a minimum of three weeks before participating in experimentation.

Microsphere Protocols

For each regional blood flow determination, the left atrial VAP was accessed for injection of 15 μ m microspheres into the systemic arterial circulation. Simultaneously, the aortic VAP was accessed and a reference blood sample was withdrawn at a known rate from within the aorta as we have previously described in conscious canines [19]. Microspheres injected into the subcutaneous vascular access port traveled through the subcutaneous catheter and were released into the blood in the left atrium. In the left ventricle, the microspheres mixed with the blood and were ejected into the aorta from where they disseminated throughout the body according to the physiological distribution of blood. As the 15 μ m spheres approached capillaries, they lodged within the smallest pre-capillary arterioles based on regional tissue blood flow patterns.

The aortic blood sample acts as a reference for later determination of flow in tissues of interest. The number of counted microspheres in the reference blood sample (known) is compared to the number of microspheres that lodge and are counted in a tissue sample of interest (known). The ratio between the two sphere counts is equal to the ratio between the aortic flow (known) and flow in the tissue of interest (unknown) and provides accurate determinations of tissue specific flows in milliliters per minute per gram of tissue (ml/min/g) [24].

During the course of the study, to determine regional blood flow in the FBC, chronically instrumented conscious animals received up to eight injections of 2.25 million microspheres (18 million microspheres) over up to 19 weeks. We have previously demonstrated in this model that serial accumulation of microspheres in multiple capillary beds did not influence regional blood flow during this protocol [19].

Quantification of Fluorescent Microspheres

After euthanasia, devices and surrounding tissue structures were harvested. Tissue blocks were removed so that the skin, fascia, VAP, and muscle layer were intact for examination. Gross samples were examined and photographed. From each fibrous capsule, two sections of tissue in direct contact with the base of the device (Figure 2, Squares), and two sections of subcutaneous adipose tissue within 0.5 cm of the FBC (Figure 2, Arrows) were studied. To determine baseline flow in normal subcutaneous tissue, two sections of subcutaneous fascia were harvested from the lateral back at least 6 cm away from device implantation. Tissue and reference blood samples were sent to IMT/Stason Laboratories (Irvine, CA) for automated

digestion and counting of fluorescent microspheres using flow cytometry. Reference flows were calculated as ml/min/g.

Statistical Analysis

Flow values from the FBC, tissue within 0.5 cm of the FBC, and tissue distal to the surgical site were compared in relationship to each material type as well as between material types by paired t-tests. A p-value < 0.05 was considered statistically significant.

Results

We studied 40 subcutaneously implanted devices (20 polysulfone, 10 silicone-coated, 10 titanium) in 10 canines. Fifty-five regional blood flow determinations were made between 22 and 134 days postoperatively. Table 1 summarizes the instrumentation and number of blood flow determinations by post-operative day in each animal.

All implanted material types elicited a statistically significant increase in blood flow in the FBC as well as in subcutaneous adipose tissue within 5 mm of the fibrous capsule. Figure 3 shows mean flow values in the fibrous capsule, subcutaneous tissue immediately surrounding the fibrous pocket, and subcutaneous fascia distal to the surgical site in relationship to each device material. Blood flow in the FBCs was 0.24 ± 0.31 (mean \pm SD) ml/min/g surrounding polysulfone devices, 0.23 ± 0.18 ml/min/g surrounding silicone-coated devices, and 0.21 ± 0.15 ml/min/g surrounding titanium devices. Blood flow in adipose tissue contiguous with the FBCs was 0.14 ± 0.18 ml/min/g surrounding polysulfone devices, 0.07 ± 0.1 ml/min/g surrounding silicone-coated devices, and 0.09 ± 0.11 ml/min/g surrounding titanium devices. Control blood flow in normal subcutaneous tissue distal to the surgical site was 0.08 ± 0.9 ml/min/g.

Blood flow within FBCs increased from normal adipose flow values to similarly elevated levels for each device material and these increases were not statistically different between materials. However, Figure 4 illustrates that the different device materials did elicit statistically different flow values in adipose tissue within 5 mm of the FBC. Specifically, blood flow in subcutaneous fascia surrounding the polysulfone FBCs increased significantly as compared to normal subcutaneous blood flow of 0.09 ± 0.09 ($p < 0.0081$) and as compared to blood flow in subcutaneous fascia surrounding silicone ($p = 0.0017$) and titanium ($p = 0.0174$) FBCs. Blood flow values in subcutaneous fascia surrounding silicone and titanium devices were not statistically different from normal subcutaneous blood flow or from each other.

Figure 5 illustrates the time-course of blood flow changes for each device material over the course of the study. Measured blood flows within the FBC surrounding polysulfone and silicone devices were initially elevated and decreased over the course of the study toward chronically elevated values slightly above normal subcutaneous blood flow. Blood flow in tissues surrounding titanium devices followed a slightly different time-course in which flow values remained low for the duration of the study. The gross appearance of FBCs are illustrated in Figure 6 which shows examples of polysulfone (P) and titanium (T) VAPs *in situ* at the time of explantation. By far the largest and most developed vascular trees are concentrated around the polysulfone VAP and to a lesser extent around the titanium VAP. Histologically, the FBCs consisted of dense fibrous tissue with varying degrees of chronic inflammation which tended to be animal specific. The histological vascularity of the tissues typically corresponded to the gross findings illustrated.

Discussion

It has become progressively more important to characterize and understand pathophysiological responses of living tissue to implanted objects. Increasing knowledge of molecular and cellular physiology and the development of nanofabrication techniques heralds the development of a new generation of nanoengineered and highly biocompatible biomaterials. Novel nanomaterials engineered to mimic the dimensions and molecular structures of cellular surface proteins would be expected to interact with cellular structures and thereby activate or suppress cellular responses as designed [reviewed in 20]. Therefore, the anticipated arrival of biomimetic materials warrants multidisciplinary study of conventional biomaterials and the development of methods for characterizing biocompatibility.

With this goal in mind, we have developed a chronically instrumented large animal model of subcutaneous device implantation and microsphere delivery for serial determination of regional blood flow in conscious canines [19]. This model allows clinically relevant insights into microcirculation during long-term pathophysiological, pharmaceutical, and environmental influences on regional arterial blood flow patterns. Similar to the techniques described by Rudolph and Heymann [22] and Makowski et al. [23], small diameter microspheres injected into the left atrium distribute throughout the body and become trapped in vascular beds of interest based on regional blood flow patterns. Using this model, the purpose of the present study was to quantify regional blood flow within the FBC and determine if devices of clinically relevant size constructed from different materials provoke quantifiably different blood flow within the FBC and subcutaneous fascia immediately surrounding the device.

In the past, investigators have studied implantable biomaterials and evaluated histological features of the foreign-body response [1,5,7,9–11,13–16], as well as semi-quantitatively measured blood flow in the FBC with $^{133}\text{Xenon}$ clearance, infrared thermography, and laser doppler flowometry [16]. However, these studies have been performed in relationship to implants of millimeter dimensions or smaller and not devices of clinically-relevant size. Devices used in human medicine are typically centimeters long and wide. Such devices trigger a more substantial foreign-body response than experimental, small-dimension flat sheets. Nonetheless, the results from these studies have indicated that the nature of the FBC is highly sensitive to physical characteristics of the implanted device [2,4–8]. Features of the implanted material such as porosity or specific molecular moieties may influence fibrous capsule thickness, density, and microvessel growth. To further advance understanding of the flow patterns within tissues surrounding implanted foreign-objects, we measured blood flow in the FBC and adipose tissue surrounding implants of centimeter dimensions.

Standard deviations for blood flow within the FBCs and surrounding tissues were relatively large. Animal to animal response differences may have accounted for these differences. It was noted that some individual animals had more localized chronic inflammation, less fibrotically dense FBCs, and more vascularity typically had larger blood flow values. In these animals, a more robust foreign-body and chronic inflammatory response may have amplified angiogenesis and maintained elevated blood flow during the construction and maintenance of the FBC. This observation is the focus of additional study in our laboratory. Additionally, device proximity and/or multiple devices implanted in the same general location may have influenced healing around multiple devices and could account for the large range of observed blood flows.

The time-course of measured blood flows within the FBC surrounding each device material were not similar in shape. After the initial surgical insult and recovery period, blood flow was elevated in foreign-body capsules surrounding polysulfone and silicone devices but remained

relatively constant in foreign-body capsules surrounding titanium devices for the duration of the study. Figure 5 illustrates average blood flow within the FBCs surrounding each device material and the shape of the flow-time relationship during the construction and maintenance of the FBC. This time-course analysis suggests that device materials may differentially influenced the healing process chronically over weeks.

Our results demonstrate that implanted devices increase blood flow in the FBC as well as surrounding adipose tissue and that device material may influence regional flow patterns. Titanium, a biologically-inert material, and silicone, an inorganic and minimally biologically active biocompatible material, produced a chronic foreign-body response characterized by statistically significant increases in blood flow in the FBC and small but statistically insignificant increases in blood flow in adipose tissue immediately surrounding the FBC. However, polysulfone, a carbon based polymer presumed to be more biologically active, provoked a greater pathologic response which included more substantial increases in blood flow in the FBC and statistically significant increases in adipose blood flow surrounding the FBC. As illustrated in Figure 6, the greatest vascularity was observed around the polysulfone VAP and to a lesser extent around the titanium VAP.

These results suggest that different biomaterials may elicit differential histopathologic and immunologic responses from the foreign object within the FBC as well as in tissues immediately surrounding the FBC. Although we did not measure systemic or local cytokine or chemokine levels or quantify cell populations, it is possible that the individual biomaterials may have affected immunologic, tissue-repair, and/or microvessel growth pathways differently. Recruitment and activation of fibroblasts, collagen deposition and matrix remodeling, and neovascularization and microvessel development within the developing FBC may be influenced by gross or molecular characteristics of the surface of the implanted devices. For example, during the foreign-body response, Hevin and SPARC, two homolog matricellular proteins, mediate the architecture of the collagenous FBC. These matricellular proteins inhibit angiogenesis in the FBC and may be influenced by implant material and microgeometry [21]. Likely, characteristics of different materials preferentially activate or inhibit cellular mechanisms that influence remodeling pathways and govern the ultimate architecture of the FBC. Additional studies are needed to investigate these pathways.

For devices with sensory or delivery systems in which diffusion is necessary, microvessel proliferation within the FBC may be important for device function. The fibrous matrix of a FBC increases the overall mass-transfer resistance of the tissue and impedes the diffusion of analytes to and from the device into the surrounding vasculature [1,4]. As an example for future investigation and application, an understanding of the blood flow patterns within the FBC may help to calibrate delivery or sensory algorithms within devices with sensory and/or delivery functions.

Additional studies with old and new biomaterials and devices are needed to further quantify the time course of flow pattern changes in the FBC, systemic and local cytokine and chemokine levels, and roles of cell types and molecules that mediate neovascularization, angiogenesis, and the construction of the FBC. Further characterization of the foreign-body response will lead to more biocompatible materials designed to activate or suppress cellular responses as designed.

Limitations

Microsphere injections were not performed after the same number of post-operative days in each animal. We have shown that blood flow values change over the course of tissue remodeling and formation of the ultimate chronic FBC. These differences in time may have

influenced results and may account for the large standard deviations noted in the blood flow measurements.

An initial baseline blood flow value was not available from the site of device implantation. Prior to instrumentation surgery, microspheres could not be injected to establish baseline subcutaneous blood flow before device implantation. Similarly, microspheres could not be injected post-operatively until animals had recovered from surgery and were not under the influence of analgesics which may alter vascular tone and influence systemic or regional hemodynamics. This limitation of the model precludes collection of a baseline flow value at the site of implantation and determination of regional blood flow patterns during the initial, acute foreign-body response before cellular infiltration and FBC maturation.

Implanted devices were different in shape and size. It has been shown that device dimensions may affect the nature of the FBC and may have influenced flow values within the FBCs.

During the course of this study, these chronically instrumented animals underwent additional and unrelated experimental protocols in which the implanted devices were used for data acquisition related to the study of inhaled air pollution (data not shown). Although we do not believe that these exposures influenced the present study, we acknowledge this as a limitation.

Notwithstanding these limitations, the current study contains several strengths including the use of a clinically relevant, conscious, large animal model, and a longitudinal repeated-measures study design. Our results suggest that this model may be implemented to evaluate local blood flow within the FBC surrounding devices of clinically-relevant size and that device material may provoke quantifiably different blood flow within the FBC and surrounding subcutaneous fascia.

Conclusions

We have developed a chronically instrumented, conscious large animal model to quantify blood flow within foreign-body capsules. Surgically implanted subcutaneous devices of clinically relevant size elicit increases in blood flow in the foreign-body capsule as well as surrounding fascia. Device material may influence regional flow patterns.

Acknowledgments

The authors acknowledge and thank Gregory Wellenius ScD, Ichiro Akiyama MD, Brent Coull PhD, Edgar Diaz MD, Kazunori Okabe MD, Joy Lawrence PhD, Sandra Verrier, Lani Lee, Tracy Katz, Jeffrey Pettit, Mark Long and the Harvard veterinary staff for their support and assistance during the instrumentation and maintenance of these animals and during the preparation of this manuscript. Joe Carlos of IMT Laboratories was instrumental in the processing of microsphere tissue samples.

Additionally, this work has been accepted in partial fulfillment for the degree of Master of Liberal Arts in Biotechnology, Harvard University Extension School, Cambridge, MA (CRB).

Funding Sources

This study was supported by grants RD831917, R827353, and R832416 from the US Environmental Protection Agency, and by grants R01 ES12972 and ES00002 from the National Institute of Environmental Health Sciences. Its contents are solely the responsibility of the authors and do not necessarily represent the official views of NIEHS, NIH, or the EPA.

References

1. Wood RC, LeCluyse EL, Fix JA. Assessment of a model for measuring drug diffusion through implant-generated fibrous capsule membranes. *Biomaterials* 1995 Aug;16(12):957–959. [PubMed: 8562786]

2. Taylor SR, Gibbons DF. Effect of surface texture on the soft tissue response to polymer implants. *J Biomed Mater Res* 1983 Mar;17(2):205–227. [PubMed: 6841364]
3. Thomson HG. The fate of the pseudosheath pocket around silicone implants. *Plast Reconstr Surg* 1973 Jun;51(6):667–671. [PubMed: 4705323]
4. Anderson JM, Niven H, Pelagalli J, Olanoff LS, Jones RD. The role of the fibrous capsule in the function of implanted drug-polymer sustained release systems. *J Biomed Mater Res* 1981 Nov;15(6):889–902. [PubMed: 7309770]
5. Beahan P, Hull D. A study of the interface between a fibrous polyurethane arterial prosthesis and natural tissue. *J Biomed Mater Res* 1982 Nov;16(6):827–838. [PubMed: 6757256]
6. Matlaga BF, Yasenchak LP, Salthouse TN. Tissue response to implanted polymers: the significance of sample shape. *J Biomed Mater Res* 1976 May;10(3):391–397. [PubMed: 1270456]
7. Ward WK, Slobodzian EP, Tiekotter KL, Wood MD. The effect of microgeometry, implant thickness and polyurethane chemistry on the foreign body response to subcutaneous implants. *Biomaterials* 2002 Nov;23(21):4185–4192. [PubMed: 12194521]
8. Davila JC, Lautsch EV, Palmer TE. Some physical factors affecting the acceptance of synthetic materials as tissue implants. *Ann N Y Acad Sci* 1968 Jan;146(1):138–147. [PubMed: 5238629]
9. Clark H, Barbari TA, Stump K, Rao G. Histologic evaluation of the inflammatory response around implanted hollow fiber membranes. *J Biomed Mater Res* 2000;52(1):183–192. [PubMed: 10906691]
10. Ravin AG, Olbrich KC, Levin LS, Usala AL, Klitzman B. Long-and short-term effects of biological hydrogels on capsule microvascular density around implants in rats. *J Biomed Mater Res* 2001 May 1;58(3):313–318. [PubMed: 11319747]
11. Setzen G, Williams EF 3rd. Tissue response to suture materials implanted subcutaneously in a rabbit model. *Plast Reconstr Surg* 1997 Dec;100(7):1788–1795. [PubMed: 9393477]
12. Hu WJ, Eaton JW, Ugarova TP, Tang L. Molecular basis of biomaterial-mediated foreign body reactions. *Blood* 2001 Aug 15;98(4):1231–1238. [PubMed: 11493475]
13. Rezzani R, Rodella L, Tartaglia GM, Paganelli C, Sapelli P, Bianchi R. Mast cells and the inflammatory response to different implanted biomaterials. *Arch Histol Cytol* 2004;67(3):211–217. [PubMed: 15570886]
14. Pier, GB.; Lyczak, JB.; Wetzler, LM. *Immunology, infection, and immunity*. ASM press; 2004.
15. Vince DG, Hunt JA, Williams DF. Quantitative assessment of the tissue response to implanted biomaterials. *Biomaterials* 1991 Oct;12(8):731–736. [PubMed: 1724732]
16. Bouet T, Schmitt M, Desuzinges C, Eloy R. Quantitative in vivo studies of hyperemia in the course of the tissue response to biomaterial implantation. *J Biomed Mater Res* 1990 Nov;24(11):1439–1461. [PubMed: 2279980]
17. Bartoli CR, Akiyama I, Godleski JJ, Verrier RL. Long-term pericardial catheterization is associated with minimum foreign-body response. *Catheter Cardiovasc Interv* 2007 August;70(2):221–227. [PubMed: 17632787]
18. Bartoli CR, Okabe K, Akiyama I, Verrier RL, Godleski JJ. Technique for implantation of chronic indwelling aortic access catheters. *J of Invest Surg* 2006 Nov–Dec;19(6):397–405. [PubMed: 17101609]
19. Bartoli CR, Okabe K, Akiyama I, Godleski JJ. Repeat microsphere delivery for serial measurement of regional blood perfusion in the chronically instrumented, conscious canine. *J Surg Res* 2008 Mar; 145(1):135–141. [PubMed: 17632127]
20. Kao WJ. Evaluation of protein-modulated macrophage behavior on biomaterials: designing biomimetic materials for cellular engineering. *Biomaterials* 1999 Dec;20(23–24):2213–2221. [PubMed: 10614928]
21. Barker TH, Framson P, Puolakkainen PA, Reed M, Funk SE, Sage EH. Matricellular homologs in the foreign body response: hevin suppresses inflammation, but hevin and SPARC together diminish angiogenesis. *Am J Pathol* 2005;166(3):923–933. [PubMed: 15743803]
22. Rudolph AM, Heymann MA. The circulation of the fetus in utero. Methods for studying distribution of blood flow, cardiac output and organ blood flow. *Circ Res* 1967;21(2):163–184. [PubMed: 4952708]

23. Makowski EL, Meschia G, Droegemueller W, Battaglia FC. Measurement of umbilical arterial blood flow to the sheep placenta and fetus in utero. Distribution to cotyledons and the intercotyledonary chorion. *Circ Res* 1968;23(5):623–631. [PubMed: 5693914]
24. Hale SL, Alker KJ, Kloner RA. Evaluation of nonradioactive, colored microspheres for measurement of regional myocardial blood flow in dogs. *Circulation* 1988 Aug;78(2):428–434. [PubMed: 3396179]

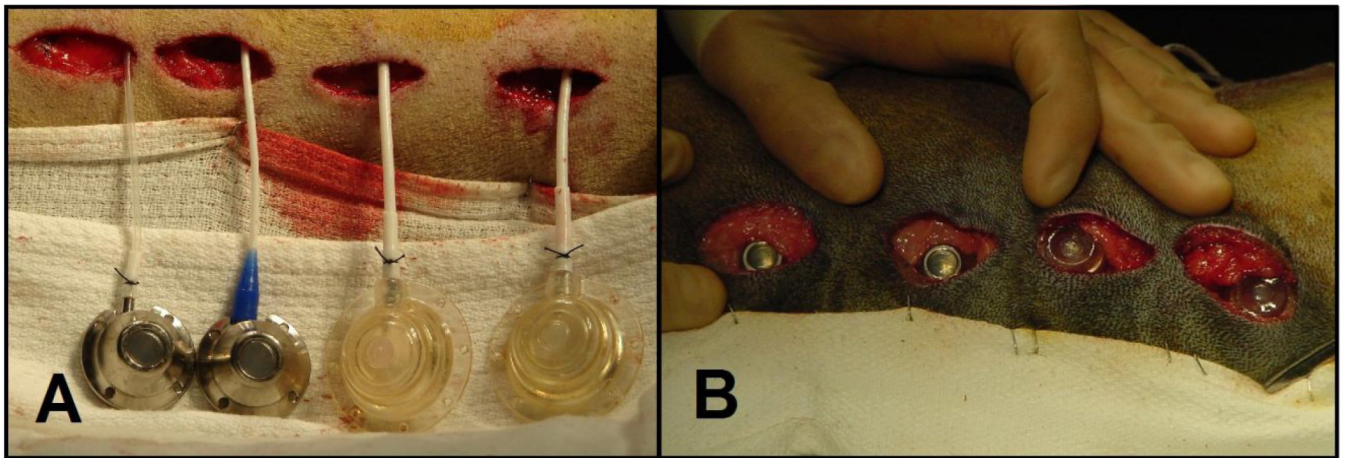


Figure 1. Titanium (right) and polysulfone (left) vascular access ports were implanted subcutaneously in the back and buried in multi-layers in the fascia. These devices served the dual purpose for delivery of microspheres into the left heart and as the implanted test device around which foreign-body capsular blood flow was repeatedly determined.

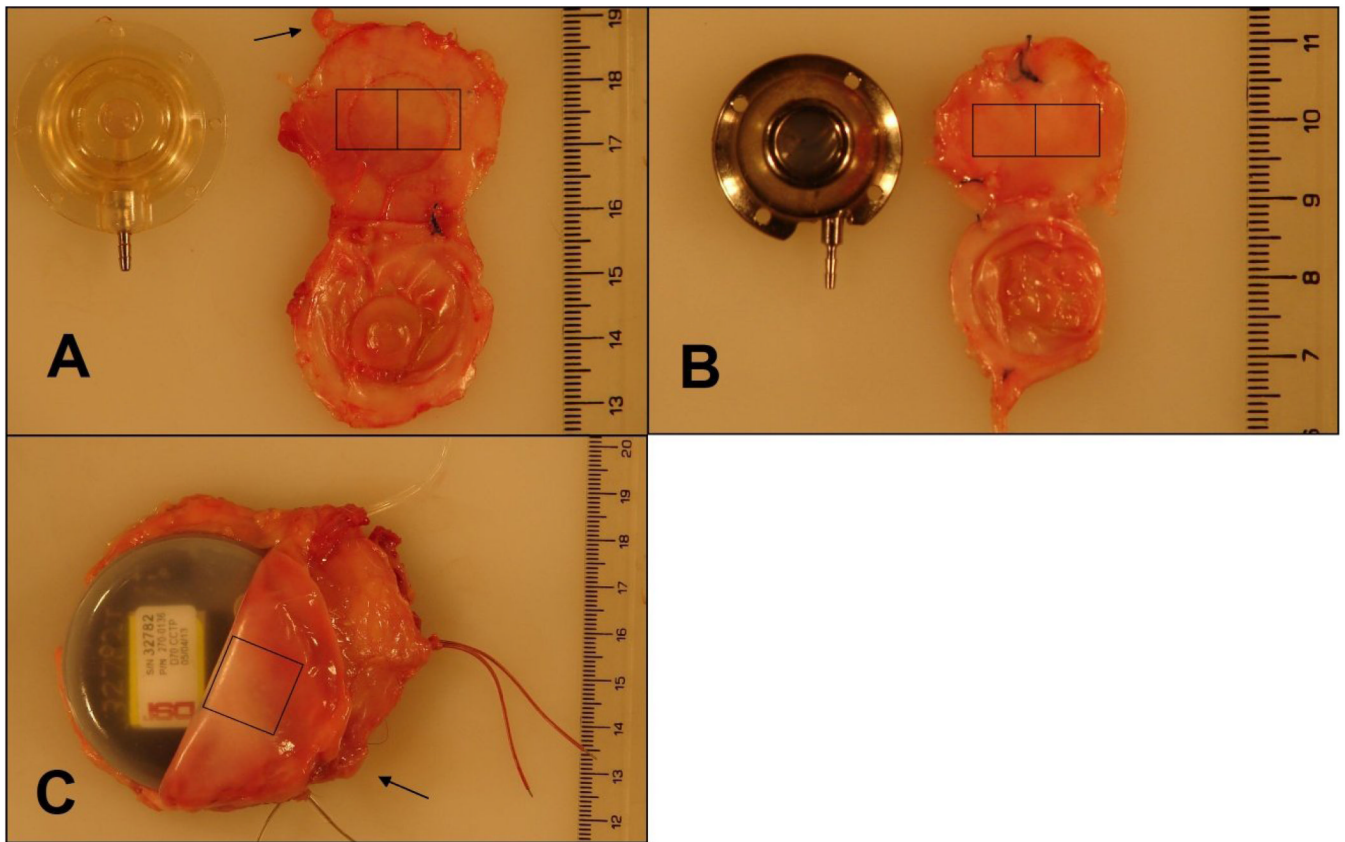


Figure 2. After euthanasia, devices and surrounding tissue structures were harvested. From each fibrous capsule, two sections of tissue in direct contact with the base of the device (boxes denote approximate locations of tissue samples), and two sections of subcutaneous adipose tissue within 0.5 cm of the capsule (arrows denote example noncapsular subcutaneous fascia) were studied. **A:** Polysulfone vascular access port (VAP) and surrounding capsule. **B:** Titanium VAP and surrounding capsule. **C:** Silicone-coated telemetry device.

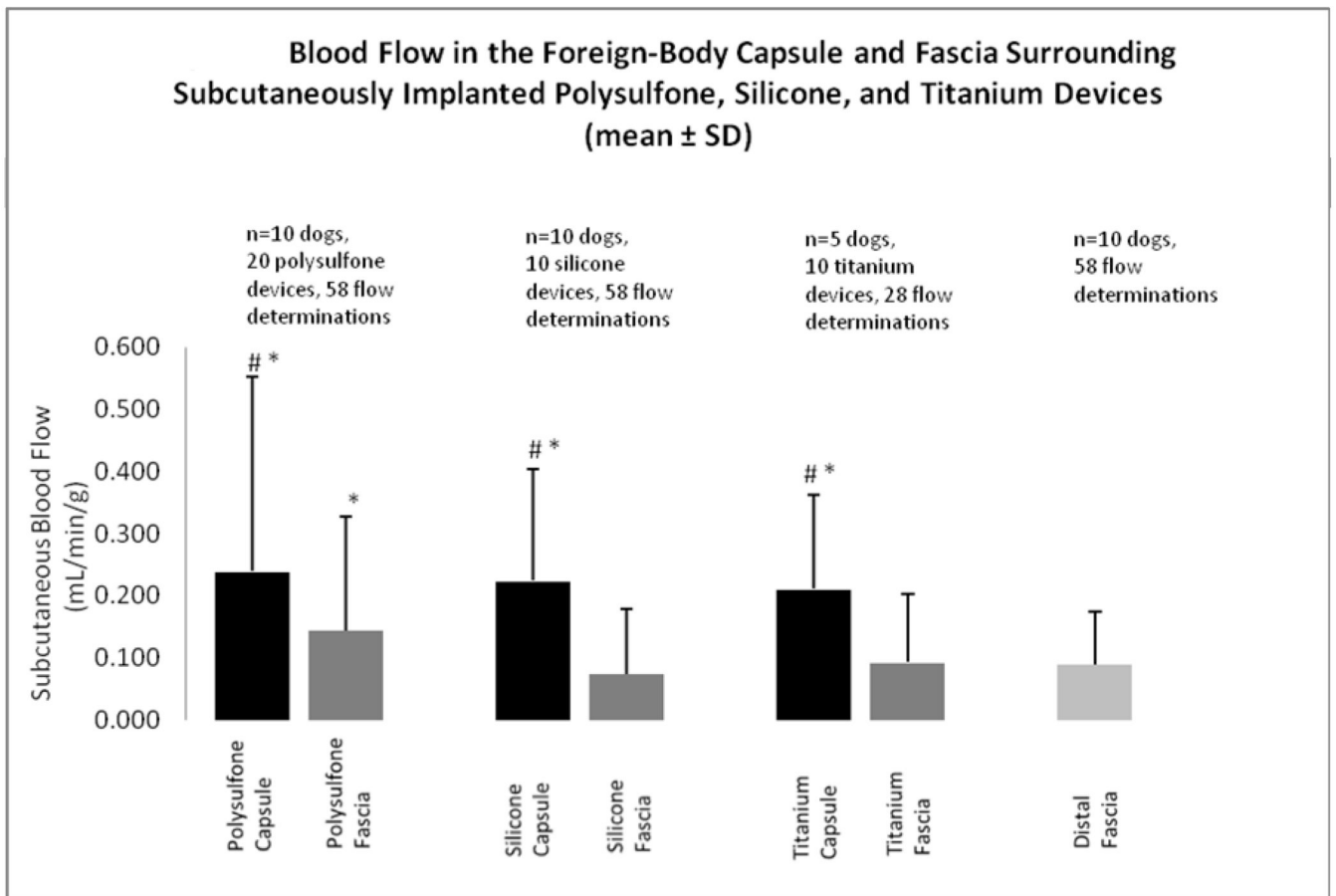


Figure 3. Blood flow in the foreign-body capsule and fascia surrounding subcutaneously implanted polysulfone, silicone, and titanium devices (mean \pm SD).
 # $p < 0.01$ vs. fascia blood flow for that material
 * $p < 0.001$ vs. distal fascia blood flow

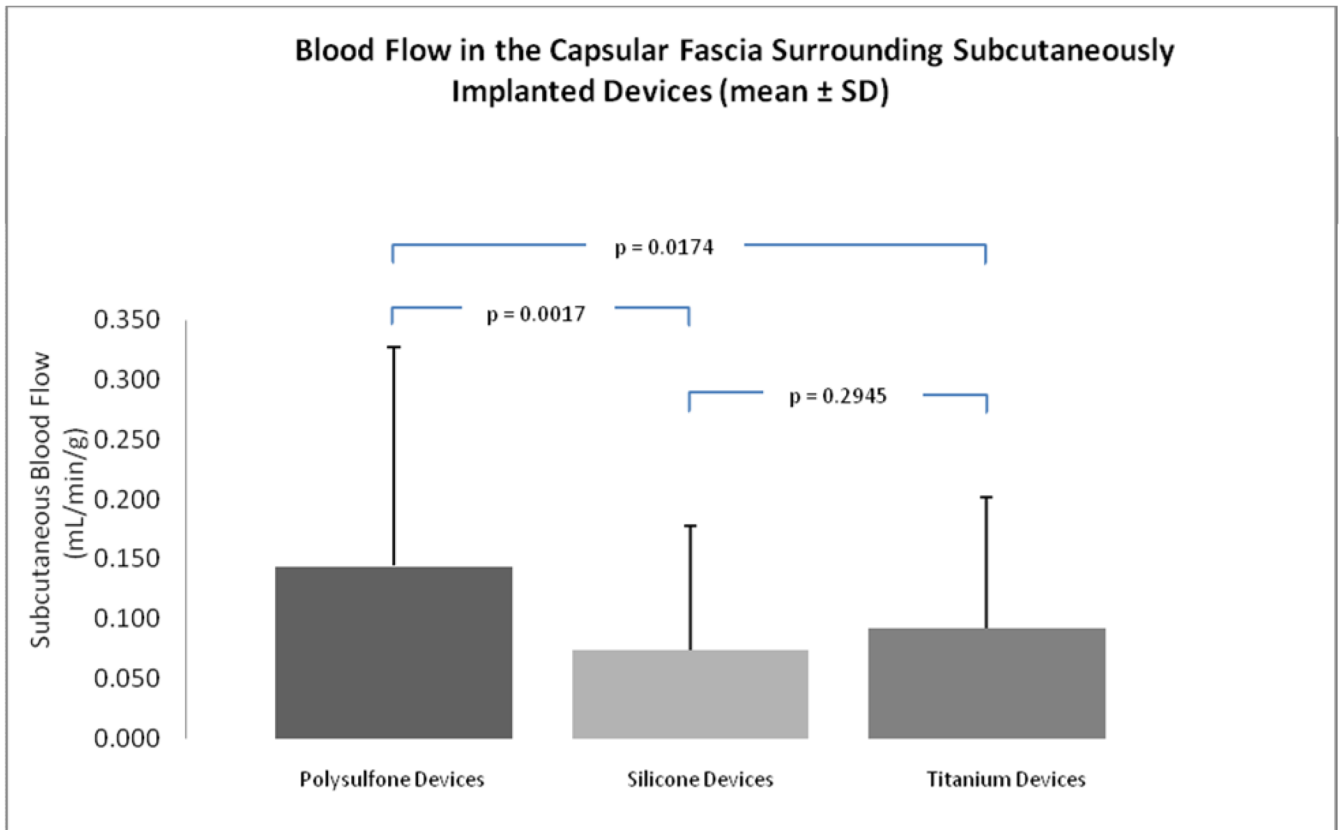


Figure 4. Blood flow in the capsular fascia within 5mm of the foreign-body capsule surrounding subcutaneously implanted devices (mean \pm SD).

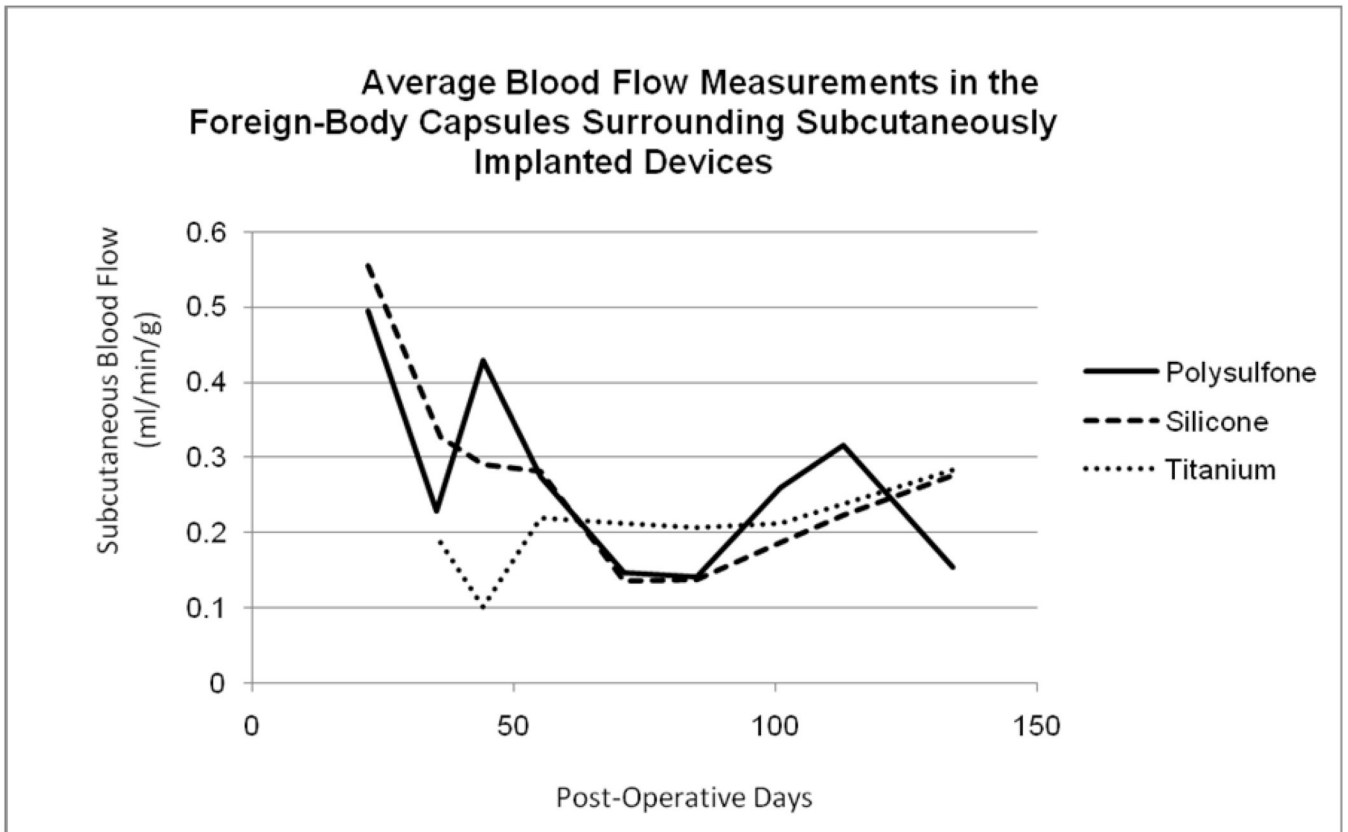


Figure 5.

The time-course of measured blood flow within the FBC surrounding each device material. After surgery and recovery, blood flow in foreign-body capsules surrounding polysulfone and silicone devices was elevated and decreased toward chronically elevated values slightly above normal subcutaneous blood flow. Blood flow in tissues surrounding titanium devices followed a different time-course in which flow values remained low for the duration of the study.

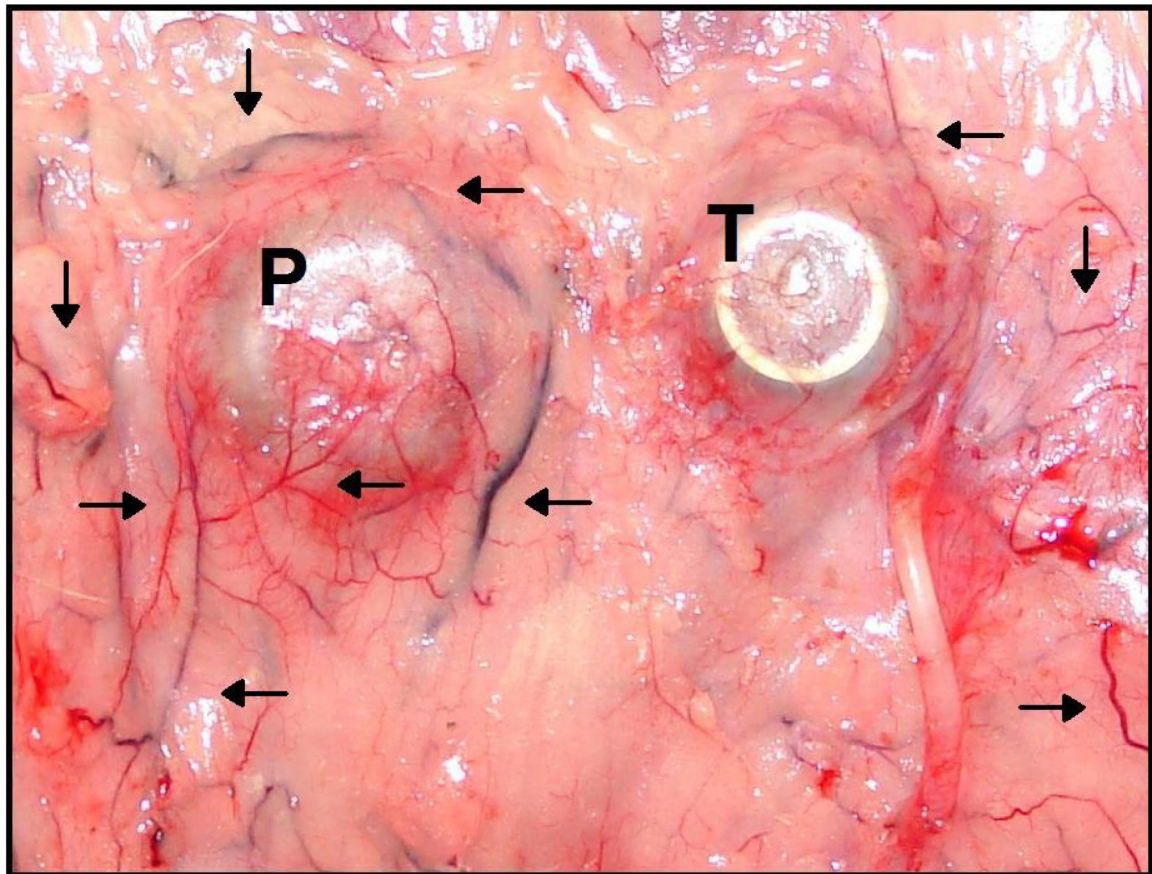


Figure 6.

In situ example polysulfone (P) and titanium (T) vascular access ports (VAPs) at the time of explanation. Large and branched vessels seem to congregate around the polysulfone VAP and to a lesser extent around the titanium VAP. These *de novo* vascular structures in close proximity to the devices underscore the role of neovascularization in foreign-body capsule development. The increased presence around the polysulfone device further demonstrates differential foreign-body response to individual device materials.

Table 1

Instrumentation and flow determinations in each animal.

Dog	Weight (kg)	Flow Determinations by Post-Surgical Day	Ports Implanted		
			Polysulfone	Titanium	Silicone Coated
Gi	14.2	4 Determinations (day 85, 106, 113, 118)	2		1
La	14.6	6 Determinations (day 22, 26, 30, 42, 49, 54)	2		1
Pa	16.5	5 Determinations (day 23, 27, 31, 50, 55)	2		1
Rh	15.3	7 Determination (day 33, 35, 38, 55, 62, 64)	2		1
Ma	14.7	6 Determination (day 31, 33, 36, 53, 60, 62)	2		1
Wi	16	6 Determinations (day 28, 35, 41, 50, 62, 91)	2	2	1
Be	15.1	4 Determinations (day 28, 35, 41, 50)	2	2	1
Ab	16	3 Determinations (day 84, 120, 134)	2	2	1
Co	16.5	6 Determinations (day 41, 44, 49, 77, 89, 105)	2	2	1
Va	18.2	8 Determinations (day 50, 55, 71, 78, 85, 92, 99, 101)	2	2	1